Cryogenics 96 (2018) 99–107

Contents lists available at ScienceDirect

Cryogenics

journal homepage: www.elsevier.com/locate/cryogenics

Research paper

Numerical study on the heat transfer characteristics of oscillating flow in cryogenic regenerators

Shuangtao Chen[a], Qian Huang[a], Menglin Liang[b], Houlei Chen[b], Liang Chen[a,*], Yu Hou[a]

[a] State Key Laboratory of Multiphase Flow in Power Engineering, Xi'an Jiaotong University, Xi'an 710049, PR China
[b] Technical Institute of Physics and Chemistry, Chinese Academy of Sciences, Beijing 100190, PR China

ARTICLE INFO

Keywords:
Regenerator
Pulse-tube cryocooler
Oscillating flow
Convective heat transfer

ABSTRACT

The heat transfer characteristics of oscillating flow in regenerator have significant impacts on the system performance of regenerative cryocoolers such as pulse tube, Stirling and G-M type cryocoolers. In this paper, the hydrodynamics and heat transfer in porous media featuring periodically configured arrays of cylinders are simulated under periodically oscillating flow conditions. The effects of operating parameters including working frequency, velocity amplitude and location on the heat transfer coefficient are evaluated. The simulation results reveal that the Nusselt number is significantly different between steady and oscillating flow conditions with the magnitude strongly depending on the oscillation frequency and velocity amplitude. A correlation for the cycle averaged Nusselt number is proposed, which yields deviations of 7% from the simulation results of the oscillating flow in the cylinder array.

1. Introduction

With the rapid development of space technology and superconducting device, demand for cryogenic refrigerators keeps rising. Traditional Stirling and G-M type cryocoolers have been widely used in the cooling of space detectors. Considering the cryocooler's operating life and reliability, pulse tube type cryocooler shows priority due to the advantage of no-moving parts in the cold end [1,2]. Stirling, G-M and pulse tube type cryocoolers belong to regenerative refrigerator [3] in which the working fluid features an oscillating flow condition [4]. Seume et al. [5] defined such flow condition as the fluid is doing reciprocating motion in a tube with the zero net mass delivered along the axial line. The periodically reversed flow direction leads to a zero mean velocity but a time-dependent transient velocity, making the boundary layer development and the heat transfer characteristics of oscillating flow different from that of the unidirectional steady flow [6,7].

In regenerative refrigerators, the regenerator is the key component where the periodically heat transfer between cold and warm fluid is conducted. Unlike traditional heat exchangers, the cold and warm fluids flow through the same channel and exchange heat with solid matrix directly in regenerators [8]. To improve the performance of refrigeration, the regenerator fillers should have a large heat transfer area, a large heat capacity, small axial heat conduction, a small pressure drop and a small empty volume. Wire packing, as shown in Fig. 1, is the most popular type among the three commonly used types in cryocoolers [9] (the other two types are spherical particles and gas gaps) due to its excellent heat transfer efficiency, simple geometry, easy manufacturing and low cost.

Most experimental measurements were mainly performed for the steady flow conditions [10], and only a few experimental studies were under the oscillating flow conditions. Hsu et al. [11] studied the velocity and pressure drop under the steady and oscillating flow (limited to low frequency) through the porous media of wire packing. The experimental results showed that the oscillating flow friction factors were similar to the steady ones, indicating that the friction factor for the low frequency oscillating flow in porous media can be assumed to be that of the steady flow. Nam and Jeong [12] experimentally investigated the regenerator flow resistance and ineffectiveness under the operating condition of cryocoolers. Fast response hot wire anemometers and high frequency pressure sensors were used to measure the local instantaneous velocity, pressure and temperature at the inlet and outlet of the regenerator with 200 mesh stainless screens. The thermodynamic features at both ends of the regenerator were characterized. Based on the obtained maximum pressure amplitude and enthalpy, the friction factor and ineffectiveness of the regenerator were calculated. Roberts and Desai [13] carried out experiments similar to the work by Nam and Jeong but with a regenerator consisting 400 mesh stainless steel screens. The above-mentioned studies showed that the correlations for

* Corresponding author.
E-mail address: liangchen@mail.xjtu.edu.cn (L. Chen).

https://doi.org/10.1016/j.cryogenics.2018.10.012
Received 4 May 2018; Received in revised form 25 September 2018; Accepted 24 October 2018
Available online 25 October 2018

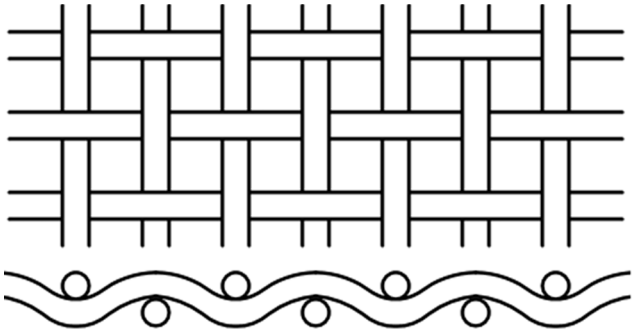

Fig. 1. Geometry structure of wire packing.

steady flow were not always suitable for the oscillating flow, indicating the need of a detailed research on the heat transfer of high frequency oscillating flows in porous media.

The experiments mentioned above were performed on the regenerator structure with the characteristic length above millimeters. For the local oscillating flow and heat transfer through the sub-millimeter structure of wire packing regenerator, the direct experimental measurement or visualization is currently unavailable due to the difficulty in obtaining temperature and velocity data from micron-sized regenerator fillers [14]. Numerical simulation presents an effective alternative to study the porous media with complex and non-uniform structures. For instance, the porous media composed of periodic arrays of regular-shaped structures such as arrays of square or circular cylinders.

Guo et al. [15] numerically studied the pulsating flow and heat transfer in a circular pipe filled with porous media, finding that the Nusselt number increased monotonically with an increase in the porous layer thickness. Kim and Ghiaasiaan [16] investigated the flow friction under laminar oscillating flow in a porous media with square arrays. The velocity and pressure variations were obtained for a porosity ranging from 0.64 to 0.84 at a flow pulsating frequency of 40 Hz with the phase shift between velocity and pressure waves also assessed. Pathak and Ghiaasiaan [17] further simulated the heat transfer in incompressible laminar oscillating flows within porous media with arrays of square cylinders, a structure similar to the work by Kim and Ghiaasiaan. The results showed that the average Nusselt number and the dimensionless thermal dispersion rate decreased as the oscillating frequency increased at a given Reynolds number and porosity. Correlations for the average Nusselt number and dimensionless thermal dispersion were further derived. Using the same simulation model, Mulcahey, Pathak and Ghiaasiaan [18] studied the relations between Nusselt number, friction factor and the location of a particular tube with a pulsating frequency ranging from 0 to 80 Hz and a Reynolds number from 50 to 100. Correlations incorporating the influence of frequency, porosity and location on the friction factor and Nusselt number were obtained. Pathak, Mulcahey and Ghiaasiaan [18] extended the study to investigate the difference in heat transfer between steady flow and periodic flow in porous media. For frequencies of 0–60 Hz, the Darcy permeability, Forchheimer and Nusselt number were obtained within a domain of 75% porosity, and significant difference was found between steady flow and oscillating flow. The above studies showed the importance of a pore-level investigation on heat transfer characteristics of oscillating flow in porous media. The model of square block array is an attempt to simplify the complicated structure of porous media, and it clearly shows the flow through a small number of unit cells. But the shape of square is obviously different from the appearance of wire screens. Moreover, the relation between the cycle-average Nusselt number and the governing parameters has not been established for the oscillating flow in a cryogenic regenerator.

In this paper, a 2D model is established to simulate the flow and heat transfer characteristics of oscillating flow in a screen type regenerator. The model shows good agreement with empirical correlations under steady state conditions. For the oscillatory state, the effects of working frequency, velocity amplitude and location on heat transfer coefficient are studied, and a correlation for the cycle averaged Nusselt is proposed. The findings and results in this work provide important guidelines for the design and optimization of cryogenic regenerators.

2. Numerical model

2.1. Simulation model

The wire packing used in regenerators is piled with layers of woven metal mesh. A complete model would require a complex 3D mesh requiring prohibitive computational time. Instead, the 2D staggered cylinder array is adopted, as shown in Fig. 2 with a wire diameter $d = 0.03$ mm and distances $s_1 = 0.0635$ mm, $s_2 = 0.0522$ mm. Compared with the 3D wire packing, the simplified 2D model has the same features in structure, which provides a useful approach to study the heat transfer through the solid matrix. Considering the symmetrical structure, a characteristic unit cell, illustrated in Fig. 2, is used as the calculation domain. Each unit is bounded by a fluid inlet, a fluid outlet, two heat transfer surfaces and four fluid edges. To make sure the flow is fully developed, 9 such unit cells are modeled. An extension is adopted after the fluid inlet to make sure that the velocity inlet boundary condition is far enough from the first unit cell with negligible pressure effects. Another extension was used before the fluid outlet to avoid flow reversal at the pressure outlet boundary. The length of extensions after the inlet and before the outlet is 0.2 mm.

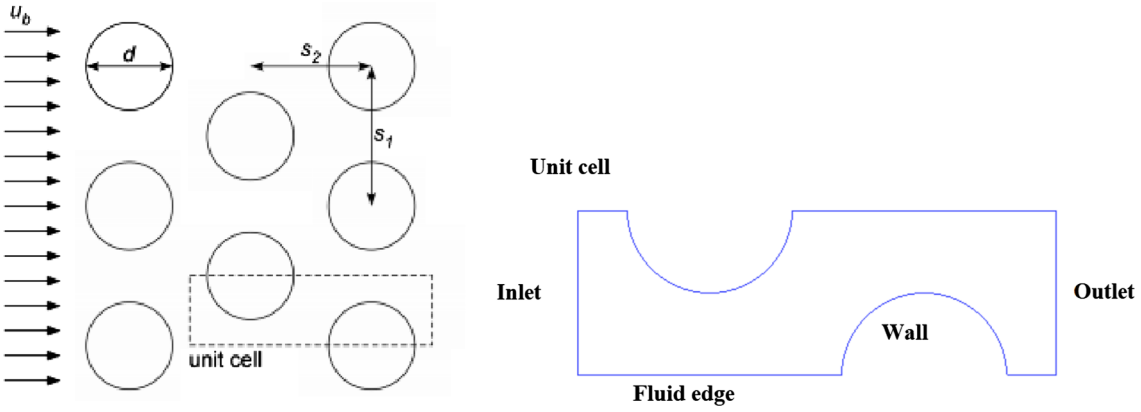

Fig. 2. The 2D model of wire packing and a basic unit.

The governing equations for the mass, momentum and energy conservations are shown in Eqs. (1)–(3).

$$\frac{\partial u_j}{\partial x_j} = 0 \tag{1}$$

$$\frac{\partial u_i}{\partial t} + \frac{\partial}{\partial x_j} u_i u_j = -\frac{1}{\rho_f}\frac{\partial P}{\partial x_i} + \frac{\partial}{\partial x_j} v_f \left(\frac{\partial u_i}{\partial x_j} + \frac{\partial u_j}{\partial x_i}\right) \tag{2}$$

$$\rho_f c_{pf}\left(\frac{\partial}{\partial_t} + \frac{\partial}{\partial x_j} u_j T\right) = \frac{\partial}{\partial x_j}\left(k_f \frac{\partial T}{\partial x_j}\right) \tag{3}$$

The inlet velocity calculated from the cold end mass flow rate is utilized as the inlet boundary condition, and the outlet pressure is as the outlet boundary condition. The walls are defined as no-slip walls at a constant temperature. Other fluid edges are symmetrical considering the flow and structure characteristics. The temperature range for the 9 unit cells is small in practice, but the temperature difference of 20 K is used between the inlet fluid and the solid surface. The wall temperature is 80 K which cools down the fluid with inlet temperature of 100 K. For the unsteady simulation, the velocity and pressure waves are simplified as time-varying sine waves, which can be modelled using UDF (standing for User-Defined Functions). The inlet velocity is expressed as $u = u_{max} sin(2\pi ft)$. Given the fact that a phase difference of 30 degree between pressure and velocity waves can improve the performance, the expression of outlet pressure is $p = p_{max} sin(2\pi ft + \pi/6)$.

2.2. Simulation parameters

The CFD software ANSYS Fluent 13.0 is used to solve the mass, momentum and energy conservation equations for a domain consisting of 9 unit cells is simulated. Considering the small temperature range, the physical properties of the working fluid helium are assumed as constants with density $\rho = 15.974\ kg/m^3$, heat capacity $c_p = 5249.4$ J/kg K, thermal conductivity $k = 0.069$ W/mK and viscosity $\mu = 9.2922 \times 10^{-6}$. The SIMPLE algorithm is used to solve the discretized governing equations. The following residuals are used for convergence check: 10^{-4} for k and ε, 10^{-5} for continuity, x and y velocities, and 10^{-6} for energy equation. A time step of 10^{-4} s is used for the unsteady simulation, which is one order of magnitude smaller than the value of minimum grid length divided by the fluid velocity and satisfies the convergence requirement. The flow is defined as fully developed for oscillating flow when the difference in physical properties of neighboring cycles are smaller than 0.1%. At least eight cycles are needed to achieve the fully-developed flow condition. All these simulations are run at an operating pressure of 3 MPa.

The choice of laminar or turbulence model is critical for simulating flows in porous media. According to the previous study [18], the approximate critical porous media Reynolds number for laminar-turbulent transition is 1600, where Re_m is defined by:

$$\mathrm{Re}_m = \frac{1 + \sqrt{1-\varepsilon^{1/2}}}{(1-\varepsilon)\varepsilon^{1/6}} \frac{d_s \rho u}{\mu} \tag{4}$$

$$d_s = \frac{6V_p}{S_p} \tag{5}$$

where V_p and S_p are the volume and surface area of a spherical blockage. The blockages investigated here are circular tubes for which $V_p = \pi d^2/4$ and $S_p = \pi D/2$. Substituting the specified values of ρ, μ and d_s, Re_m corresponding to the porosity of 0.7 is determined by $\mathrm{Re}_m \approx 14.862\mathrm{Re}$.

On the assumption that laminar flow requires $Re_m < 1600$, we use the critical Reynolds number $Re_{crit} = 107$ as the criteria for laminar or turbulence flow. The dependency on grid size was analyzed using structured grids of 120,000, 140,000, 160,000 and 180,000 and grid-independent solution was achieved for grid number over 140,000 indicated by a negligible temperature reduction (0.5%).

2.3. Similarity analysis

The studies on flow and heat transfer using similar principle requires properly chosen non-dimensional analog criteria functions. Using similarity criterion to characterize heat transfer of the oscillating flows broadens the general applicability. Moreover, it reduces the number of variable considerably, and therefore benefits simulation. Based on the governing equations of unsteady compressible viscous flow, Tang et al. [14] derived the similarity criterion with the thermal similarity characterized by Reynolds number, Valensi number and Mach number and thermal similarity by Prandtl number and specific heat ratio. Furthermore, another criteria number is needed to characterize geometric similarity and porosity is a good choice for porous media in regenerators. In this work, the specific heat ratio and Prandtl number of the helium barely changes over the range of working conditions and are accordingly excluded. Mach number, a criterion characterizing the compressibility of fluid, is not considered here as the value is much less than 1 in the range of working conditions.

In oscillating flow, the mathematical expression of Reynolds number is the same as that in steady state, which is the ratio between inertia force and viscous force. As the mean velocity of the fluid is zero, the maximum velocity (u_{max}) is adopted as the characteristic velocity to calculate the Reynolds number, *i.e.* $\mathrm{Re} = \frac{u_{max} d}{\nu}$. Valensi number, also known as Kinetic Reynolds number, is the ratio of the alternating period and the time scale of viscous diffusion, which incorporates the angular frequency, *i.e.* $Va = \frac{\omega d^2}{\nu}$.

In this paper the Reynolds number and Valensi number are chosen as the similarity criterion with can be modified by changing the fluid inlet velocity and oscillating frequency, respectively, with the porosity fixed at 0.7. In order to investigate the effect of different parameters on heat transfer, the conditions of four Reynolds numbers ranging from 100 to 300 with the mass flow ranging from 5 g/s to 20 g/s, five Valensi numbers ranging from 0.005 to 0.06 with the frequency being 10 Hz, 30 Hz, 50 Hz, 70 Hz and 120 Hz, are simulated with the porosity fixed. The detailed simulated conditions are listed in Table 1. By controlling and changing the two dimensionless criteria numbers, the characteristics of heat transfer under incompressible oscillating flow through regenerators are investigated, and furthermore the correlation of periodic average Nusselt number are deduced.

Table 1
Summary of simulated conditions.

Number	Mass flow (g/s)	Re	Frequency (Hz)	Va
1	5	97.37	10	0.0051
2	5	97.37	30	0.0152
3	5	97.37	50	0.0253
4	5	97.37	70	0.0354
5	5	97.37	120	0.0608
6	10	194.75	10	0.0051
7	10	194.75	30	0.0152
8	10	194.75	50	0.0253
9	10	194.75	70	0.0354
10	10	194.75	120	0.0608
11	15	292.12	10	0.0051
12	15	292.12	30	0.0152
13	15	292.12	50	0.0253
14	15	292.12	70	0.0354
15	15	292.12	120	0.0608
16	20	389.49	10	0.0051
17	20	389.49	30	0.0152
18	20	389.49	50	0.0253
19	20	389.49	70	0.0354
20	20	389.49	120	0.0608

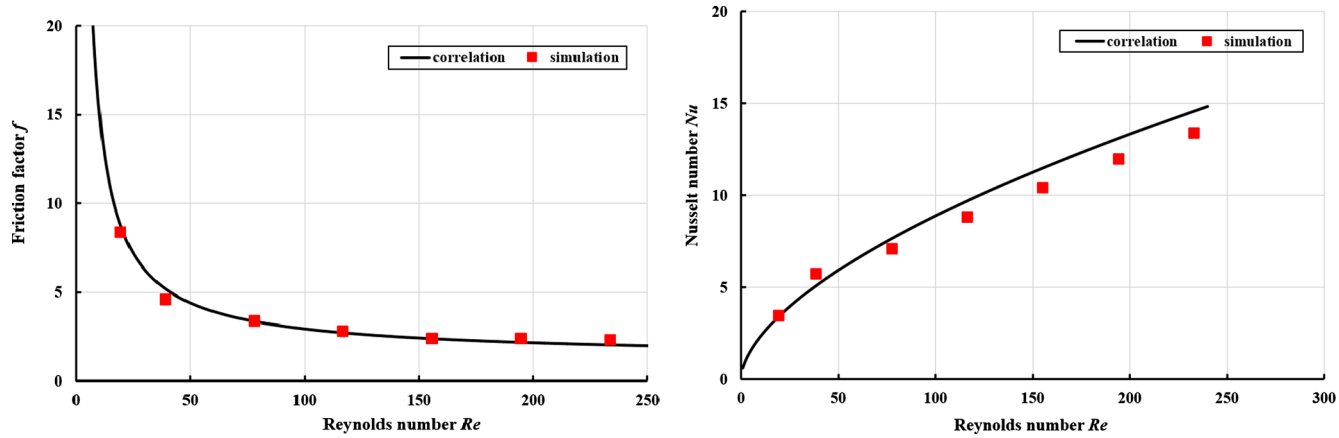

Fig. 3. Comparison of friction factor and Nusselt number between the simulation results at porosity ε = 0.7 and the correlation predictions under steady state conditions.

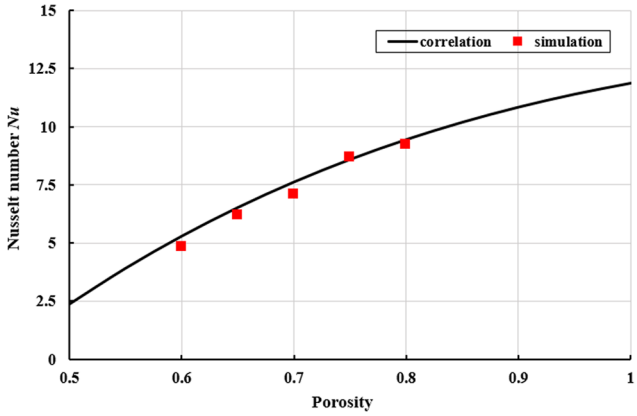

Fig. 4. Comparison of Nusselt number under different porosities.

3. Results and discussions

3.1. Model validation

The simplified 2D model was first validated by comparing the friction factor and Nusselt number with empirical correlations under steady flow conditions. The correlations, shown in Eqs. (6) and (7), were derived by Barron R F [19] based on experimental results under the condition of one-way steady flow in wire packing.

$$Nu = [1.415 - 2.490(1-\varphi)]\mathrm{Re}^{0.517+0.236(1-\varphi)}\mathrm{Pr}^{\frac{1}{3}} \tag{6}$$

$$f = \frac{132}{\mathrm{Re}}(1 + 0.0213\mathrm{Re}^{0.88}) \tag{7}$$

The friction factor is calculated using Eq. (8), where ΔP is the pressure drop across the 9 unit cells, d_h is the hydraulic diameter of mesh (0.043 mm), L is the length of the 9 unit cells, and u is the inlet velocity.

$$f = \frac{\Delta P d_h / L}{1/2\rho u^2} \tag{8}$$

The Nusselt number is calculated by $Nu = \frac{hd}{k}$, where d is the wire diameter (0.03 mm) and h is determined by $h = \frac{q}{\Delta T}$. The temperature difference ΔT is the difference between mass-averaged fluid temperature and area-averaged temperature of walls. It is noteworthy that the mass-averaged fluid temperature excludes the inlet and outlet extension sections. Steady state simulations are performed under different inlet velocities and porosities (ε = 0.6, 0.65, 0.7, 0.75, 0.8), and the results of friction factor and Nusselt number are shown in Figs. 3 and 4 with an error smaller than 15%, showing good reliability of the simplified

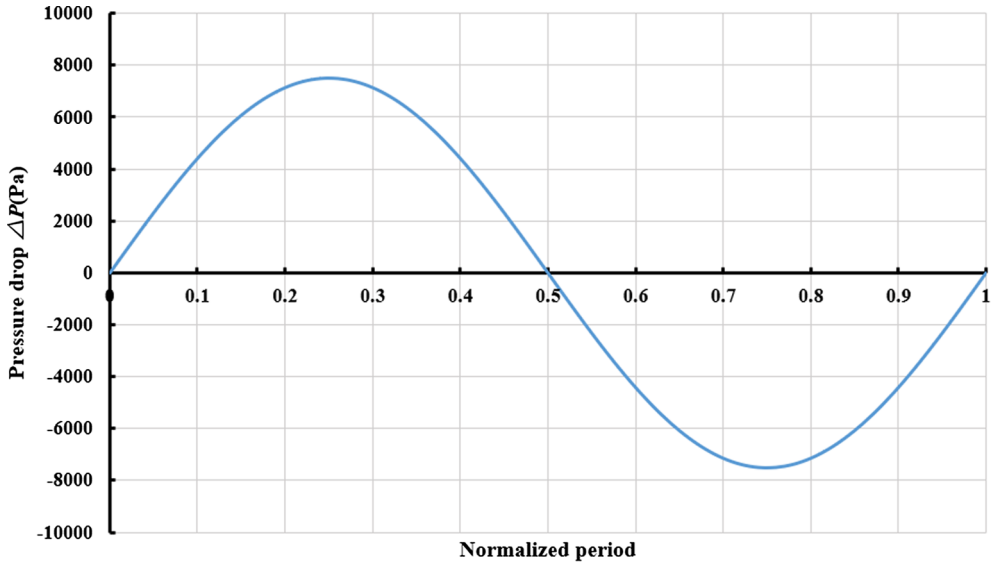

Fig. 5. The pressure drop under the case of m = 20 g/s and f = 50 Hz.

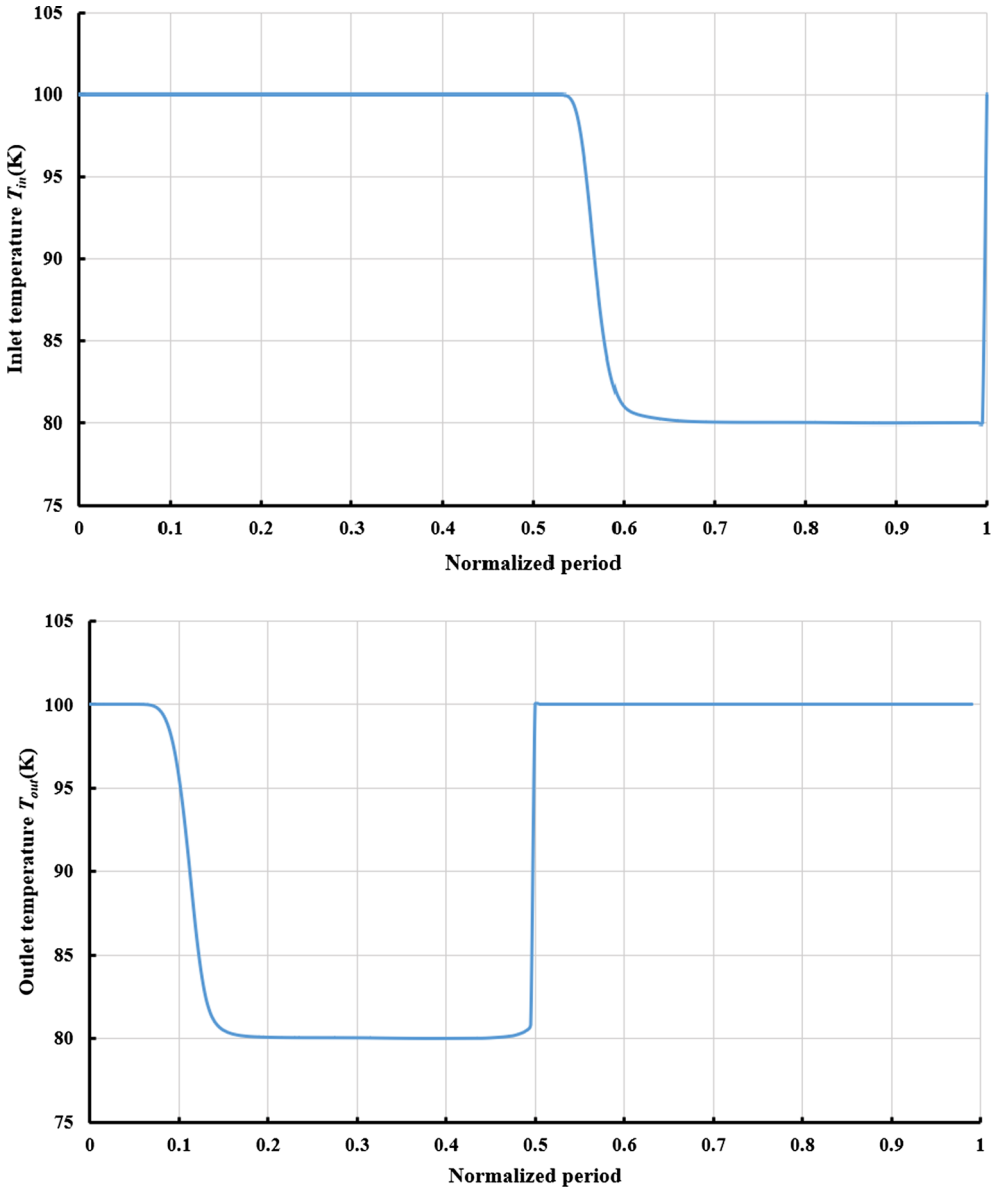

Fig. 6. The inlet and outlet temperature under the case of m = 20 g/s and f = 50 Hz.

model.

3.2. Analysis of dynamic characteristics and flow distribution

The working fluid is subject to oscillating in regenerators. The heat transfer in steady and oscillating flow differs greatly because the magnitude and direction of velocity change periodically in the latter. The results obtained from the various 20 cases show similar change laws of pressure, temperature and velocity. So, the important parameters and flow field development are exemplified using the case with a flow rate of 20 g/s and a frequency of 50 Hz. The pressure drop, shown in Fig. 5, is almost a sine function over time simply because of the given sinusoidal outlet pressure and the fluid incompressibility. The phase shift is not observed because the scale is at the micron level. The phase difference between the inlet and outlet pressure can be clearly recognized in the model at millimeter level.

Fig. 6 illustrates the inlet and outlet temperature at a function of time over a complete cycle. As mentioned, the inlet and outlet temperature is set as 100 K. During the first half cycle, the fluid at 100 K flows from the inlet into the region, and is cooled down to 80 K at the outlet. The inlet and outlet temperature remains unchanged until the end of a half cycle. At the beginning of the rear half cycle, the sinusoidal inlet velocity reverses the flowing direction. The fluid at 100 K flows from the outlet, and is cooled down to 80 K at the inlet. It can be seen that the outlet temperature falls from 100 K to 80 K and then remains unchanged at 80 K until the end of a half cycle. And because the mass flow is close to zero at the beginning of the half cycle, the outflow turns 80 K later than the half cycle.

The mass-averaged fluid temperature, shown in Fig. 7, reveals the fluctuating characteristics as well. At the very beginning, the temperature at the flow region drops quickly, and gradually becomes periodic later. During the first 1/4 cycle, with the increasing of the mass flow rate, more walls are needed to cool down the fluid, and thus the mass-averaged fluid temperature increases. During the 1/4–1/2 period, the mass-averaged fluid temperature decreases as the mass flow rate decreases. The trend in the next half cycle is almost the same with reversed flow direction. Slight difference between the two adjacent half cycles can be observed because the circular cylinders are arranged in a staggered manner, leading to slightly different structure between the inlet and outlet.

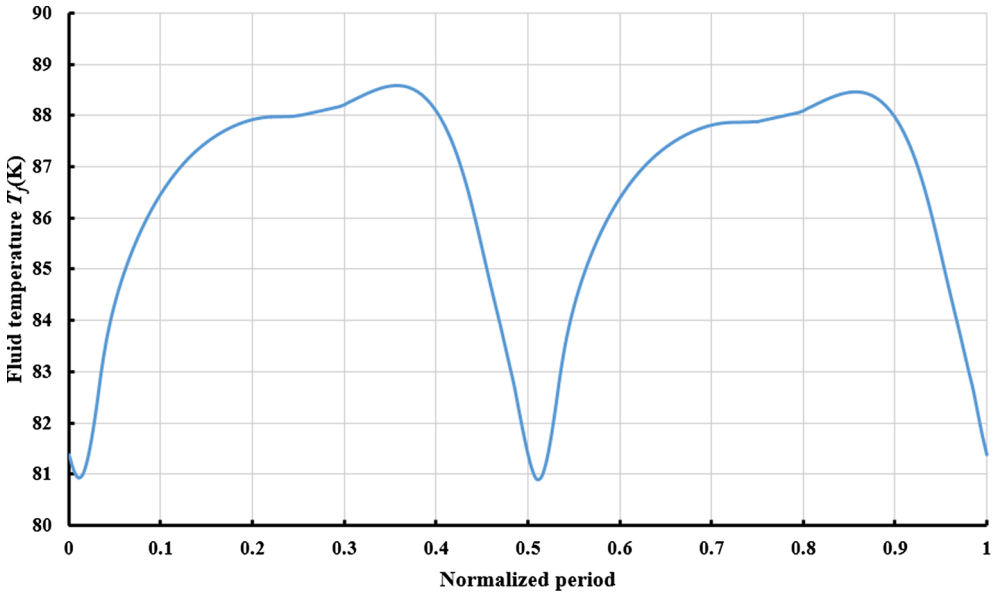

Fig. 7. The average fluid temperature under the case of m = 20 g/s and f = 50 Hz.

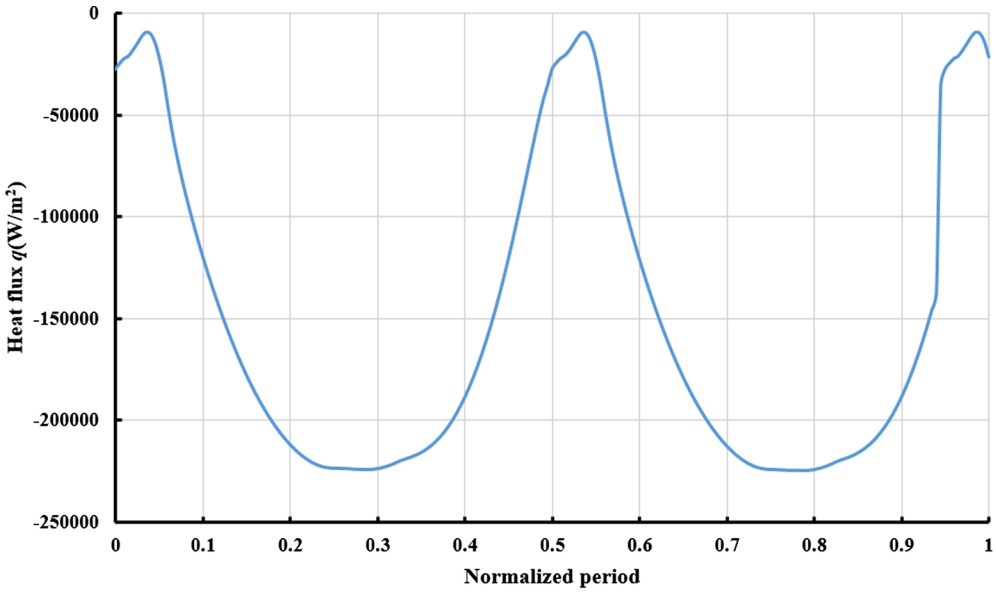

Fig. 8. The heat flux varying curve under the case of m = 20 g/s and f = 50 Hz.

The change of heat flux, shown in Fig. 8, behaves similarly to the sine waving. In the first 1/4 cycle, the heat flux increases with the mass flow rate. In the following 1/4–1/2 period, the heat flux becomes smaller as the mass flow rate decreases. In the next half period, the heat flux shows a similar trend despite the reversed flow direction. Furthermore, the two adjacent half periods are not identical, which is similar to the mass-averaged fluid temperature. The sloping trend line is the exact opposite of the one in mass-averaged fluid temperature. The heat flux falls as the average fluid temperature rises, while the heat flux goes up as the average fluid temperature goes down. The reason can be attributed to the relationship between the heat flux and temperature difference, which is the difference between the wall temperature and mass-averaged fluid temperature, resulting in the opposite changing trend of heat flux and mass-averaged fluid temperature.

Fig. 9 is a detailed illustration of the distribution of temperature, velocity and pressure at the moment of zero and maximum velocity. The temperature distribution in Figure (a) indicates that the fluid initially at 100 K is cooled down to 80 K after the 9 unit cells. When the velocity is close to zero, the temperature is distributed uniformly because heat conduction dominates the process. With the increasing of the velocity, more cooling walls are needed to cool the fluid, and the temperature distribution becomes less uniform because of the increased convective heat transfer. Comparing the two figures in Figure (b), it can be seen that the variation of velocity gets more obvious with the growth of the velocity. It is apparent that wake regions exist right behind the circles representing silk screens, which enhance the disturbance on the flow. The pressure distribution is shown in Figure (c) with variations in the flow direction and almost uniformly distributed in the perpendicular direction. As the velocity increases, the presence of wake regions disturbs the pressure distribution.

3.3. Heat transfer coefficients

The periodically averaged Nusselt number for each unit cell can be calculated based on the mass-averaged bulk temperature in each unit cell and the solid wall temperature with the expression shown in Eq.

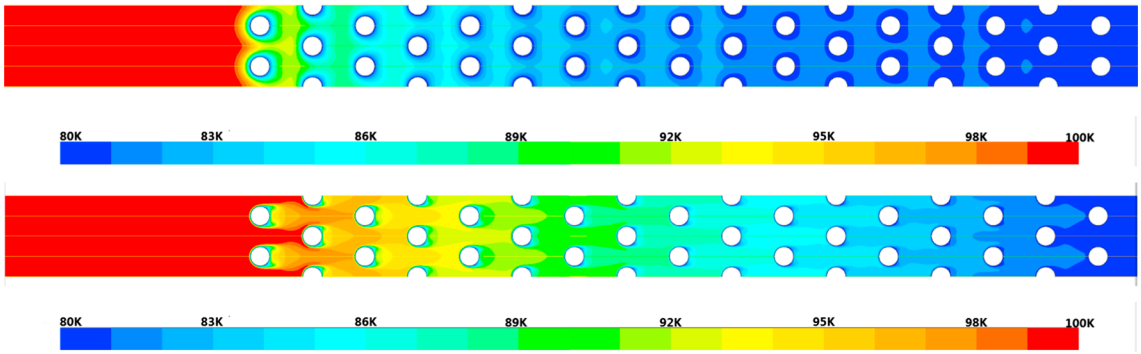

（a）The distribution of temperature

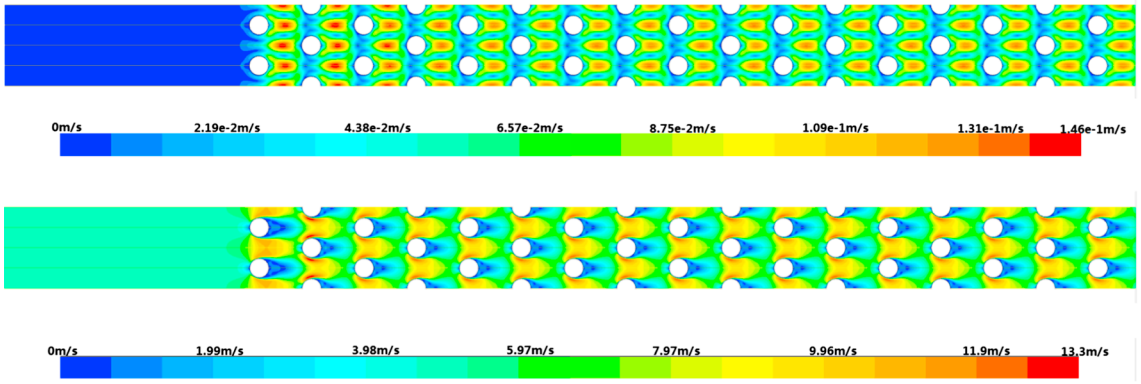

（b）The distribution of velocity

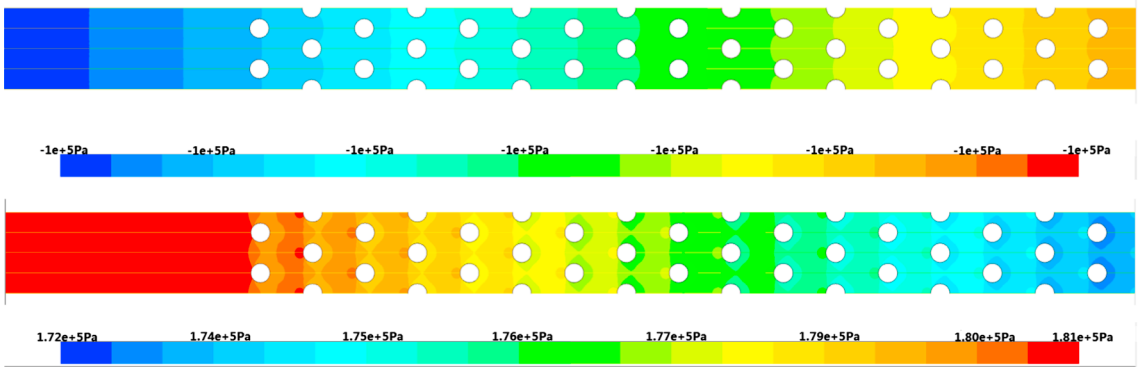

（c）The distribution of pressure

Fig. 9. The distribution of (a) temperature, (b) velocity and (c) pressure at the moment of zero and maximum velocity.

(9).

$$Nu_{cyc} = \frac{h_{cyc} d}{k} = \frac{d}{k}\frac{1}{t_{cyc}}\int_{t_0}^{t_0+t_{cyc}} h_{inst}\,dt = \frac{d}{k}\frac{1}{t_{cyc}}\int_{t_0}^{t_0+t_{cyc}} \frac{q_{inst}}{(T_w - T_{f,inst})}dt \tag{9}$$

where q is the total heat flux from the two solid walls in each unit cell, T_w is the surface temperature of the wall (80 K), and T_f is the mass-averaged temperature in the domain of each unit cell.

The cycle-average Nusselt numbers are shown in Fig. 10, showing some interesting trends. First, similar to the situation in steady flow, the heat transfer is enhanced with an increase in the Reynolds number. The Nusselt number for the first unit cell is apparently higher than that for other units and decreases with an increase in the distance from the first unit cell. This trend is consistent with the heat transfer in steady flow evolving exchanger tube bundles because of the decreased temperature difference. What's more, the flow pulsation can enhance the heat transfer between the fluid and mesh matrix, especially under high Reynolds number. The reason can be attributed to the reduced thermal boundary layer thickness in oscillatory flow. Increasing the oscillating frequency could therefore enhance the heat transfer. It can also be concluded from the figure that the effect of frequency on the cycle averaged Nusselt number is minor compared with Reynolds number, as a result of the small geometry size.

The cycle averaged Nusselt number of the middle unit cell, that is the fifth one in our model, is used to characterize the heat transfer in regenerators considering that most of the wire meshes are situated in center position. Based on the calculated results of Nusselt number, a correlation is derived when Prandlt number is 0.7. This proposed correlation can give good predictions for the oscillating flow in cryogenic regenerators in the range of Re = 100–400 and Va = 0.005–0.06.

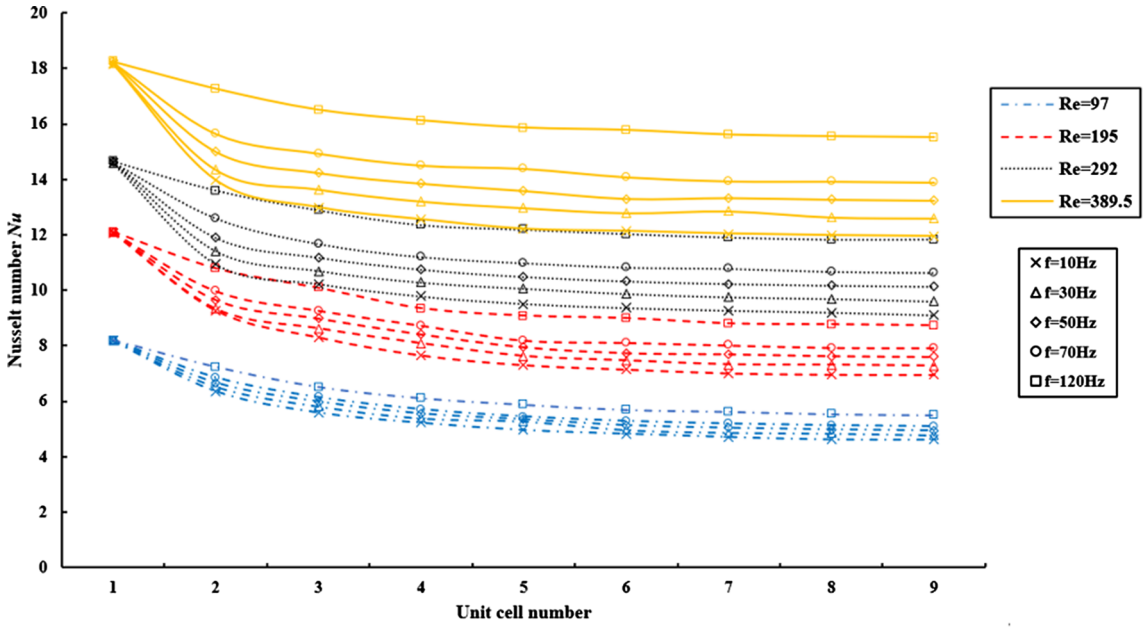

Fig. 10. Cycle-averaged Nusselt number of each unit cell for all case.

Table 2
Comparison of predictions of heat transfer coefficient by correlations with the simulation results.

Authors	Correlations	Characteristic length	Re	Frequency
Ghiaasiaan [17]	$Nu = 20.85\mathrm{Re}^{0.0873}(1-\varepsilon)^{0.4014}(e^{-0.000045Va} + 0.0001Va)$	10 mm	70–980	0–100 Hz
Mulcahey, T.I. [18]	$Nu = 0.4818\sqrt{\mathrm{Re}} + 1.928 \times 10^{-6} f\mathrm{Re} + 1.4305$	10 mm	50–200	0–80 Hz
Costa, S.C. [20]	$Nu = 1.54 + 0.29\mathrm{Re}^{0.66}$	10 mm	4–400	Steady
Fujio Kuwahara [21]	$Nu = \left[1 + \frac{4(1-\varepsilon)}{\varepsilon}\right] + \frac{1}{2}(1-\varepsilon)^{1/2}\mathrm{Re}^{0.6}\mathrm{Pr}^{1/3}$	10 mm	$10^{-2} \sim 10^{3}$	Steady
U Bin-Nun [22]	$Nu = [1 + 0.99(\mathrm{Re}\,\mathrm{Pr})^{0.66}]\varepsilon^{1.79}$	1.4–3 mm	25–61	Steady

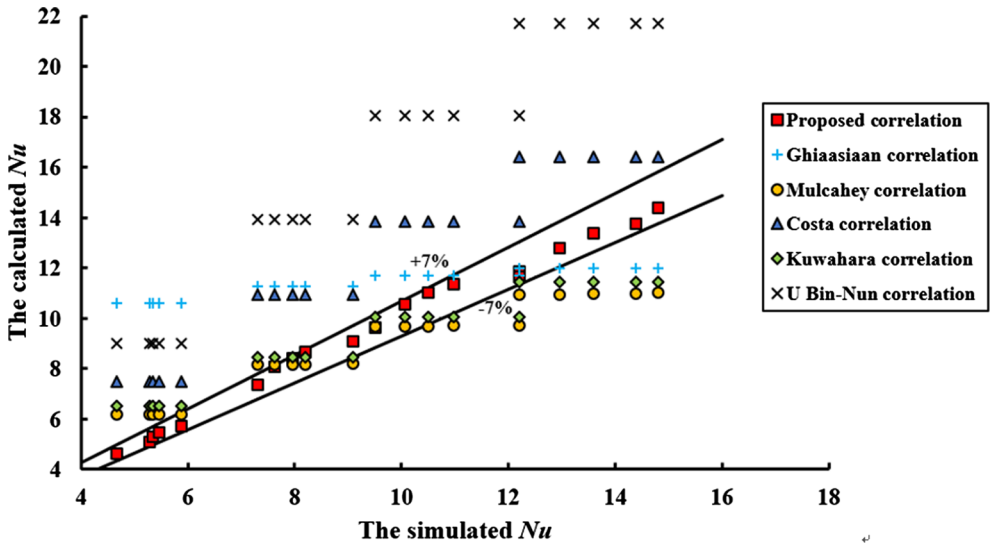

Fig. 11. The comparison between the calculated Nu and simulated Nu.

$$Nu = 0.34483\mathrm{Re}^{0.665488}\, Va^{0.08494} \tag{10}$$

Considering the effects of *Re* on the convective heat transfer coefficient, a total of 20 condition data points with different mass flow rates and working frequencies are compared with the predictions by the correlations cited from Refs. [17,18,20–22] and the formula proposed in this work, which is listed in Table 2. As shown in Fig. 11, the deviations between the simulations results and the predictions by the formula proposed in this work are smaller than 7%, while the simulation results are quite different from the predictions by the correlations cited from Refs. [17,18,20–22], especially when the frequency is high. This may be explained by the rather small characteristic length used in this work.

4. Conclusions

The simplified 2D model of circular arrays used in the current study is consistent with the experimental correlations under steady flow state. Under the oscillating state with the simplified sinusoidal mass flow rate and pressure waves, it is found that the variations of pressure drop, mass-averaged fluid temperature and heat flux over time are similar to sine functions. The effects of critical operating parameters including oscillating frequency and velocity amplitude on heat transfer are evaluated using Reynolds number and Valensi number. The results show that the cycle averaged Nusselt number of each unit cell increases with the frequency and Reynolds number and decreases with the distance away from the inlet. A correlation is proposed to predict the cycle averaged Nusselt number as a function of Reynolds number and Valensi number, and the deviations between the simulation results and the predictions are within 7%.

Acknowledgements

This work was supported by the National Nature Science Foundation of China (51706169), by the National key basic research program (613322), and Shaanxi Natural Science Basic Research Plan (2015JQ5172), China.

Appendix A. Supplementary material

Supplementary data to this article can be found online at https://doi.org/10.1016/j.cryogenics.2018.10.012.

References

[1] Jiang X, et al. An approach for estimating acoustic power in a pulse tube cryocooler. Cryogenics 2017;87:103–9.
[2] Xu J, et al. Cascade pulse-tube cryocooler using a displacer for efficient work recovery. Cryogenics 2017;86:112–7.
[3] Richardson RN, Evans BE. A review of pulse tube refrigeration. Int J Refrig 1997;20(5):367–73.
[4] Wang W, et al. Influence of the water-cooled heat exchanger on the performance of a pulse tube refrigerator. Appl Sci 2017;7(3):229.
[5] Seume J, Friedman G, Simon TW. Fluid mechanics experiments in oscillatory flow. Report. vol. 1, Final Report Minnesota Univ. Minneapolis. Dept. of Mechanical Engineering; 1992.
[6] Huang J, Liu M, Jin T. A comprehensive empirical correlation for finned heat exchangers with parallel plates working in oscillating flow. Appl Sci 2017;7(2):117.
[7] Liu X, et al. Investigation on CHF of saturated liquid nitrogen flow boiling in a horizontal small channel. Appl Therm Eng 2017;125:1025–36.
[8] Liu X, et al. Modeling of heat transfer and oscillating flow in the regenerator of a pulse tube cryocooler operating at 50 Hz. Appl Sci 2017;7(6):553.
[9] Zhang Q, et al. Numerical modeling of recuperative cryogenic matrix heat exchangers and the experimental validation. Int J Therm Sci 2016;104:330–41.
[10] Cha JJ. Hydrodynamic parameters of micro porous media for steady and oscillatory flow: application to cryocooler regenerators. Dissertations & Theses – Gradworks; 2007.
[11] Hsu CT, Fu H, Cheng P. On pressure-velocity correlation of steady and oscillating flows in regenerators made of wire screens. J Fluids Eng 1999;121(1):52–6.
[12] Nam K, Jeong S. Experimental study on the regenerator under actual operating conditions. AIP Conf Proc 2002;613(1):977–84.
[13] Roberts TP, Desai PV. Working fluid state properties measurements in medium and high frequency cryocoolers. AIP Conf Proc 2004;710:1146–53.
[14] Pathak MG. Periodic flow physics in porous media of regenerative cryocoolers. Georgia Institute of Technology; 2013.
[15] Guo Z, Sung HJ, Hyun JM. Pulsating flow and heat transfer in an annulus partially filled with porous media. Numerical Heat Transf Part A Appl 1997;40(17):4209–18.
[16] Kim SM, Ghiaasiaan SM. Numerical modeling of laminar pulsating flow in porous media. J Fluids Eng 2009;131(4).
[17] Pathak MG, Ghiaasiaan SM. Convective heat transfer and thermal dispersion during laminar pulsating flow in porous media. Int J Therm Sci 2011;50(4):440–8.
[18] Mulcahey TI, Pathak MG, Ghiaasiaan SM. The effect of flow pulsation on drag and heat transfer in an array of heated square cylinders. Int J Therm Sci 2013;64(2):105–20.
[19] Barron RF. Effect of heat transfer from ambient on cryogenic heat exchanger performance. US: Springer; 1984. p. 265–72.
[20] Costa SC, et al. Numerical study of the heat transfer in wound woven wire matrix of a Stirling regenerator. Energy Convers Manage 2014;79(79):255–64.
[21] Kuwahara F, Shirota M, Nakayama A. A numerical study of interfacial convective heat transfer coefficient in two-energy equation model for convection in porous media. Int J Heat Mass Transf 2001;44(6):1153–9.
[22] Bin-Nun U, et al. Low cost and high performance screen laminate regenerator matrix. Cryogenics 2004;44(6):439–44.